Research Square

Preprints are preliminary reports that have not undergone peer review.
They should not be considered conclusive, used to inform clinical practice,
or referenced by the media as validated information.

Action Likelihood Analysis Reveals Altered Inter-Joint Coordination After Stroke During 3D Free Exploration

Adith V. Srivatsa
adithvs2@uic.edu
University of Illinois Chicago
Arturo Ramirez
University of Illinois Chicago
Courtney Celian
Shirley Ryan AbilityLab
Valentino Wilson
University of Illinois Chicago
Bruno Borghi
Shirley Ryan AbilityLab
Adriana Cancrini
University of Illinois Chicago
Mac Camardo
University of Illinois Chicago
Naveed Reza Aghamohammadi
University of Illinois Chicago
R. James Cotton
Shirley Ryan AbilityLab
James L. Patton
University of Illinois Chicago

Research Article

Keywords: stroke, abnormal motor synergies, upper extremity, inter-joint coordination, kinematic analysis, movement distributions, action likelihood

Posted Date: November 16th, 2026

DOI: https://doi.org/10.21203/rs.3.rs-11529819/v1

License: This work is licensed under a Creative Commons Attribution 4.0 International License.
Read Full License

Additional Declarations: No competing interests reported.

Action Likelihood Analysis Reveals Altered Inter-Joint Coordination After Stroke During 3D Free Exploration

Adith V. Srivatsa[1,2,3*], Arturo Ramirez[1,3], Courtney Celian[3], Valentino Wilson[1,3], Bruno Borghi[3], Adriana Cancrini[1,3], Mac Camardo[1,3], Naveed Reza Aghamohammadi[1,3], R. James Cotton[3,4], James L. Patton[1,3]

[1*]Richard and Loan Hill Department of Biomedical Engineering, University of Illinois Chicago, Chicago, IL, USA.
[2]College of Medicine, University of Illinois Chicago, Chicago, IL, USA.
[3]Shirley Ryan AbilityLab, Chicago, IL, USA.
[4]Department of Physical Medicine and Rehabilitation, Northwestern University, Chicago, IL, USA.

*Corresponding author(s). E-mail(s): adithsrivatsa@gmail.com;
Contributing authors: aramire4@uic.edu; ccelian@sralab.org; valentinowilson93@gmail.com; bborghi@sralab.org; adri.cancrini@gmail.com; maccamardo123@gmail.com; naveed.aghamohammadi@gmail.com; rcotton@sralab.org; pattonj@uic.edu;

Abstract

Abnormal motor synergies are pathological changes in inter-joint coordination commonly observed after stroke and contribute to upper-extremity movement limitations. Their assessment is complicated by the coexistence of other motor impairments, including weakness and spasticity, and the large variability in individuals post-stroke, motivating the development of fast, quantitative approaches

to characterize movement abnormalities. Here, we investigate action likelihood analysis as a potential framework for identifying kinematic signatures associated with abnormal motor synergies. We asked neurotypical (NT) participants and individuals with a history of stroke (IwHS) to explore their dominant arm or stroke-affected arm's range of motion for two minutes. Paired distributions of joint angles and angular velocities were compared between groups using the NT group as a reference, with inter-joint correlations, regional distribution differences, and Granger causality analyses used to characterize altered coordination. The results revealed coupled inter-joint relationships in IwHS, including stronger correlations between horizontal adduction and external rotation and between humeral elevation and elbow flexion, alongside regional differences in paired distributions, and increased direction-specific temporal predictability. In contrast, the relationship between humeral elevation and external rotation remained relatively preserved under the tested conditions. Together, these findings demonstrate that action likelihoods capture joint-specific alterations in upper extremity coordination following stroke and provide converging kinematic evidence of patterns potentially associated with abnormal motor synergies. Interpretation is limited by the sample size and the heterogeneity of the IwHS group, as well as the potential contributions of coexisting motor impairments. Future work should relate distributional signatures to independently assessed deficits and functional outcomes to determine their specificity and clinical utility. Action likelihood analysis may ultimately support rapid, quantitative movement assessment and more individualized rehabilitation planning.

Keywords: stroke, abnormal motor synergies, upper extremity, inter-joint coordination, kinematic analysis, movement distributions, action likelihood

1 Introduction

Every person who has experienced a stroke faces a unique recovery from movement deficits. In many individuals with a history of stroke (IwHS), ischemic damage to the motor-related regions of the brain disrupts the corticospinal tract, which plays a primary role in transmitting voluntary motor commands to the spinal cord [1, 2]. Immediately after a stroke, this disruption can result in contralateral muscle weakness or flaccidity [3]. Although motor function often partially recovers over time, the return

of strength is frequently accompanied by persistent deficits in movement coordination and independent joint control, which substantially impact daily life [4, 5].

Abnormal motor synergies (AMS) are common after a stroke and are characterized by involuntary coupling of movements across multiple joints, limiting the ability to independently control individual joints [2]. The current proposed mechanisms imply that these synergies are the result of a greater dependence on brain stem pathways, including the reticulospinal tract after damage to the corticospinal tract [2, 6]. Newer frameworks also suggest that they could be observed in movement patterns as interactions of weakness, spasticity, and other neural changes [7]. Two characteristic upper-extremity patterns are the flexor and extensor synergies [8, 9]. The flexor synergy couples shoulder abduction with external rotation (ER), elbow flexion (EF), forearm supination, and wrist flexion; while the extensor synergy couples shoulder adduction with internal rotation, elbow extension, forearm pronation, and wrist flexion [10]. Regardless of their underlying mechanisms, these AMS may constrain independent joint movement and limit functional movement.

AMS can emerge within weeks after stroke and their severity and persistence vary substantially between individuals [11]. Although some individuals experience reductions in AMS with recovery, they may persist chronically in others. Treatment approaches that target AMS have demonstrated the potential to improve functional outcomes even in people with chronic stroke [12–14]. Given their variable recovery trajectories and responsiveness to targeted interventions, identifying and quantifying AMS early and throughout recovery may help inform more individualized interventions.

Clinicians assess upper extremity AMS through subjective observation, manual muscle testing, and comprehensive clinical assessments such as the Fugl-Meyer Assessment of the Upper Extremity (FMUE) [15, 16]. Though these assessments provide valuable information about motor impairment, they can be time-intensive and dependent on clinical judgment [15]. Repeated assessments may be particularly challenging when patients are evolving between sessions, and time devoted to assessment can reduce time available for therapeutic interventions. Objective and efficient approaches for quantifying abnormal movement patterns could complement existing clinical assessments and facilitate longitudinal monitoring of recovery.

Advances in movement-sensing technology have created opportunities for more objective assessments of motor impairments. Marker-based motion capture can precisely quantify movement trajectories and changes in movement patterns over the course of rehabilitation [17, 18]. Wearable sensors, including accelerometers placed at the wrist and other joints, have shown promise for longitudinal assessment outside the clinic [19, 20]. Surface electromyography provides another approach for characterizing abnormal coordination by measuring muscle activity during gross and fine movement [21]. When combined with techniques such as non-negative matrix factorization, electromyography can identify groups of muscles that activated together across neurotypical individuals and populations with neurological impairment during a variety of activities [11]. However, these approaches can require cumbersome sensor placement, specialized lab equipment, and substantial setup time, limiting their practicality for routine clinical use. Markerless motion capture has emerged as a potential

alternative, with recent studies demonstrating that single-camera systems can provide accurate kinematic measurements while substantially reducing setup requirements [17, 22, 23]. Such systems can enable objective assessments of abnormal movement patterns without imposing demands on clinical time and resources. However, methods are still needed to translate these large quantities of kinematic data into clinically meaningful measures of abnormal motor control.

Action likelihood analysis (ALA) provides one potential framework for addressing this challenge. ALA characterizes movement as a set of probability distributions, allowing large datasets from neurotypical (NT) participants to establish a reference distribution against which movement from an individual with neurological impairment can be compared [24]. Regions in which an individual's movement distribution differs significantly from the neurotypical reference can then be identified as potential signatures of impaired motor control [25]. Previous applications of ALA using wrist-position data collected during robotic tasks or markerless movement have identified distinct and patient-specific movement patterns in IwHS [26, 27]. These studies have demonstrated that ALA can capture clinically relevant differences in movement, including differences in improvement related to patient effort, and have been used to evaluate the effects of interventions such as antigravity assistance [28, 29]. More recent work has extended ALA toward evaluating weakness and AMS during free exploration tasks [30].

Wrist position is an endpoint measure that can reflect the combined effects of multiple impairments, but it may not identify the specific joint-level mechanisms contributing to an individual's abnormal movement [31, 32]. A given change in

the reachable workspace, for example, may result from weakness, abnormal interjoint coordination, contractures associated with spasticity, or compensatory strategies. Extending ALA to joint angles and their kinematics may prove a more direct means of identifying abnormal interjoint relationships and link observed movement signatures to specific motor impairments.

Here, we investigate ALA of paired upper-extremity joint-angle kinematics in IwHS during unconstrained free exploration using markerless motion capture. We hypothesized that abnormal motor synergies will be reflected by multiple complementary signatures of interjoint coupling: increased correlations between paired joint kinematics, significant regional differences in joint-angle probability distributions between IwHS and NT participants, and directional predictability of one joint's velocity from another. We further hypothesized that these measures will provide converging evidence of the characteristic coupling between shoulder movements and elbow flexion associated with upper-extremity AMS.

2 Methods

2.1 Participants and Experimental Protocol

Twenty NT participants (26.35 ± 10.12 years, 9 male) and 37 IwHS (57.32 ± 14.00 years, 23 male) provided informed consent to participate in their respective studies, which were approved by the Northwestern University Institutional Review Board (STU00216158, STU00216062, STU00215000, STU00220740, STU00218538). Participants were eligible if they were between the ages of 18 and 80, and IwHS were

additionally required to be at least 8 months post-stroke. They were also excluded if they presented with concurrent musculoskeletal injury. A trained clinician evaluated all IwHS using the FMUE.

Prior to the above studies, participants included in this study completed a two-minute free exploration task as part of preliminary assessments. They stood approximately two meters in front of a Kinect v2 sensor (Microsoft, Redmond, WA, USA), which was used for markerless motion capture. During the free exploration task, participants were instructed to move their dominant arm (NT) or paretic arm (IwHS) through its reachable workspace while exploring a variety of movements and speeds and avoiding repetition of the same movements unless it occurred naturally.

2.2 Data Processing

The Kinect v2 estimates the three-dimensional positions of 25 body joints sampled at 30 Hz (Figure 1). Joint positions were recorded and timestamped. To account for small variations in sampling frequency, data were interpolated to a uniform 30 Hz and low-pass filtered using a second-order Butterworth filter with a 1.5 Hz cutoff frequency as shown in Figure 1 [33]. The shoulder-to-elbow and elbow-to-wrist, unit vectors, u and v, were computed as defined in Equations (1) and (2), respectively.

$$\mathbf{u} = \frac{\mathbf{p}_{elbow} - \mathbf{p}_{shoulder}}{\|\mathbf{p}_{elbow} - \mathbf{p}_{shoulder}\|} \tag{1}$$

$$\mathbf{v} = \frac{\mathbf{p}_{wrist} - \mathbf{p}_{elbow}}{\|\mathbf{p}_{wrist} - \mathbf{p}_{elbow}\|} \tag{2}$$

Using these vectors and a coordinate system with the x-axis pointing laterally, the y-axis anteriorly, and the z-axis superiorly, we calculated the angles horizontal adduction (HA), humeral elevation (HE), and internal rotation (IR) for the shoulder joint, as well as elbow flexion (EF) according to Equations (3), (4), (5), and (8).

$$\mathrm{HA} = \mathrm{atan2}(u_y, u_x) \tag{3}$$

$$\mathrm{HE} = \mathrm{atan2}\left(u_z, \sqrt{u_x^2 + u_y^2}\right) \tag{4}$$

$$\mathrm{EF} = \mathrm{atan2}\left(\|\mathbf{u} \times \mathbf{v}\|, \mathbf{u} \cdot \mathbf{v}\right) \tag{5}$$

We cast shoulder IR as the angle between the forearm projected onto the plane perpendicular to the humerus and the projection of the global vertical axis $z = (0, 0, 1)$ onto the same plane. The projection forearm vector, $v_\perp$, and the projected vertical vectors, t, were computed using Equations (6) and (7), respectively, and used to estimate IR in Equation (8).

$$\mathbf{t} = \frac{\mathbf{z} - (\mathbf{z} \cdot \mathbf{u})\mathbf{u}}{\|\mathbf{z} - (\mathbf{z} \cdot \mathbf{u})\mathbf{u}\|} \tag{6}$$

$$\mathbf{v}_\perp = \frac{\mathbf{v} - (\mathbf{v} \cdot \mathbf{u})\mathbf{u}}{\|\mathbf{v} - (\mathbf{v} \cdot \mathbf{u})\mathbf{u}\|} \tag{7}$$

$$\mathrm{IR} = -\mathrm{atan2}\left((\mathbf{t} \times \mathbf{v}_\perp) \cdot \mathbf{u}, \mathbf{t} \cdot \mathbf{v}_\perp\right) \tag{8}$$

Shoulder IR becomes ill-conditioned when the humerus is nearly aligned with the vertical axis or when elbow flexion is less than 30°. Therefore, IR measurements

were considered unreliable when $|v_\perp| < 0.50$ or $|t| < 0.1$, and these intervals were interpolated using the nearest reliable measurements.

Joint angle conventions were defined such that 0° corresponded to the lateral direction in HA, the arm hanging vertically for HE, the forearm pointing upward with the elbow flexed at 90 degrees for IR, and full elbow extension as presented in Figure 1.

We then computed the angular velocities in $\dot{q}_0 = \Delta q/dt$ for each joint angle using finite differences. Derivative boundary artifacts were identified using a robust median absolute deviation criterion. Samples exceeding $10 \cdot mad$ were classified as outliers and replaced using interpolation.

2.3 Action Likelihood Analysis

For both the IwHS and NT groups, we concatenated participant joint angle data to visualize broad patterns. To quantify these differences, we calculated the mean angle per participant for each joint and compared the group means using Welch's t-tests.

We then created two-dimensional (2D) distributions of paired joint angles for HA-IR, HA-EF, HA-HE, HE-IR, HE-EF, and IR-EF pairs which we hypothesized would uncover the presence of AMS. For each pair, we split this data into 8 bins for each joint angle, creating a $8x8$ histogram, and calculated the probability distribution using $samples_{bin}/samples_{total}$. We then quantified interjoint coupling using a probability-weighted Pearson correlation coefficient. The center of each 2D bin was treated as the corresponding pair of joint-angle values, and the probability density within each bin was used as its weight. Weighted means, covariance, and variances, were calculated across the distribution, and the weighted correlation coefficient was computed as the

covariance divided by the square root of the product of the weighted variances. We repeated the above process for angular velocity data, generating paired $8x8$ histograms and weighted correlation coefficients. Correlation coefficients of the joint angles and angular velocities were compared between groups using Welch's t-test. These coefficients from the IwHS group were related to level of impairment using Pearson's correlation.

We quantified regional differences in the distributions by comparing bin-level probabilities between groups for both angular and angular velocity $8x8$ binned paired histograms. We took the probabilities in each bin for all participants of a group and compared each bin's probabilities between groups, using Welch's t-test with the Benjamini-Hochberg procedure to control for the false discovery rate. We noted bin-level significance as $alpha = 0.05$.

In the NT group, we averaged the probability distributions to create a reference distribution for each pairwise distribution. We then calculated the 95% CI of probabilities in each pixel. For each IwHS, we subtracted the NT-derived reference 2D distribution from the participants' 2D distribution, creating a probability difference distribution, an example of which is provided in Figure 1. Significance was determined if the pixel probability fell outside the 95% CI.

To improve the clinical richness of these distributions, we combined the angular position distributions with the velocity direction distributions, enabling visualization of coupling patterns within joint angle space. For each bin of the $8x8$ angular position histogram, we computed the conditional probability distribution of instantaneous velocity direction, discretized into eight bins spanning 0-360°. This yields an $8x8x8$

angle-direction coupling tensor, in which each angular position bin contains a full directional probability distribution describing the movement directions associated with that joint configuration. Values within each directional distribution were derived per subject then averaged across subjects within each clinical group to produce a group-level coupling field. We then assessed the directional asymmetry within each bin of the $8x8$ histogram by calculating the difference in probability between vectors in odd and even quadrants for each participant and testing whether these differences differed from zero using one-sample t-tests, with the Benjamini-Hochberg procedure to control for the false discovery rate.

2.4 Predictive Precedence

To assess directional temporal relationships between joint movements, we performed bivariate Granger causality analyses using the time-series angular velocities of each paired joint in both directions for each participant. For each joint pair and direction, we fit a linear vector autoregressive (VAR) model to the two angular velocity time series. Candidate models included up to eight temporal lags (264ms at 30-Hz sampling rate), with the optimal lag order selected using Akaike's information criterion. Granger causality was assessed using an F-test comparing the unrestricted VAR model with a restricted model in which the lagged values of the putative predictor were excluded. The resulting F-statistic quantified the evidence that past values of one joint's angular velocity improved prediction of the other joint's angular velocity.

F-statistics were compared between NT and IwHS groups using the Wilcoxon rank-sum test because the resulting distributions were non-normal and right-skewed. Within

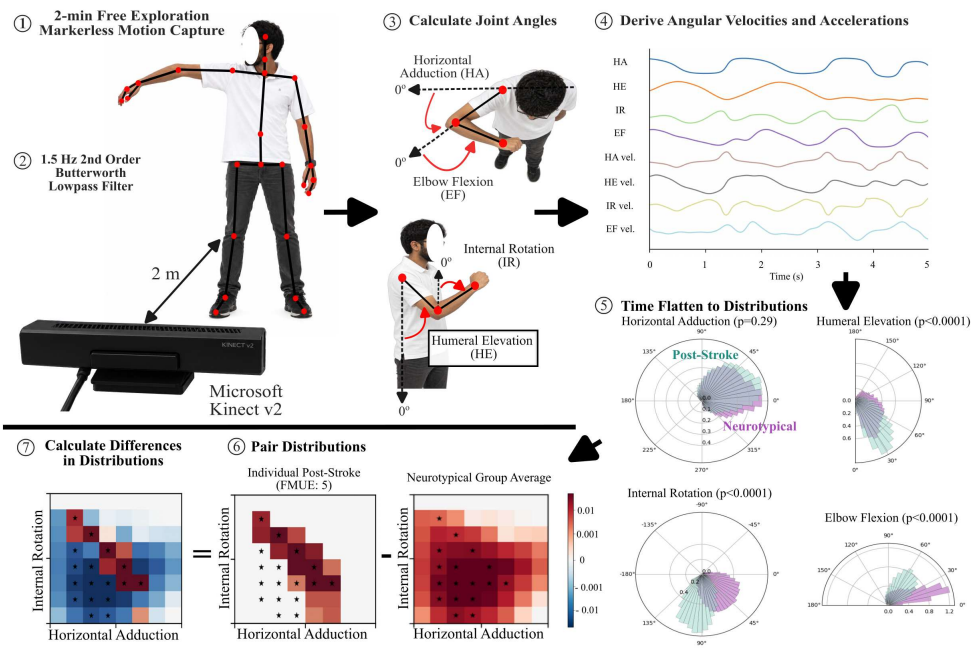


Fig. 1 Data processing pipeline. An individual's joint position data is filtered, and we compute upper extremity joint angles. Angular and angular velocity time-series data are time-flattened to achieve distributions. In step 5, we present group differences in the joint angle distributions. These are paired between joints, where we compare probabilities in specific bins and correlations. In step 7, we illustrate the internal rotation and horizontal adduction 2D distribution differences between an IwHS with FMUE of 5 and the NT group. Red represents overrepresented areas, and blue underrepresented. Stars indicate significant group differences.

the IwHS group, associations between F-statistics and FMUE were assessed using Pearson correlation. When F-statistics differed significantly between groups in both directions, F-statistics were compared between directions within each group using the Wilcoxon signed-rank test. Statistical significance was assessed at $\alpha = 0.05$.

3 Results

During free exploration, IwHS did not differ from NT participants in horizontal adduction ($28.49° \pm 13.74°$ vs. $24.27° \pm 15.32°$, $p = 0.31$) as shown in Figure 1. IwHS had lower humeral elevation angles than the NT group ($52.48° \pm 14.87°$ vs. $69.27° \pm 11.80°$, $p < 0.0001$), and IwHS were more internally rotated, on average, compared to the NT group ($87.35° \pm 18.28°$ vs. $50.70° \pm 9.79°$, $p < 0.0001$). IwHS also had higher elbow flexion than the NT group ($63.39° \pm 17.79°$ vs. $45.00° \pm 12.67°$, $p < 0.0001$).

3.1 Horizontal Adduction Coupling with Internal Rotation

Participants in the IwHS group exhibited significantly lower weighted correlations between HA and IR joint angles than those in the NT group (median [IQR]: -0.45 [-0.55 - -0.22] vs. 0.05 [-0.09 - 0.14], respectively; $p < 0.0001$; Figure 2b). HA-IR angular velocity correlations were similarly lower in IwHS than in NT participants (median [IQR]: -0.42 [-0.53 - -0.28] vs. 0.05 [-0.11 - 0.13], respectively; $p < 0.0001$). Neither joint angle nor angular velocity correlations were associated with FMUE scores (joint angles: $r = 0.02$, $p = 0.90$; angular velocities: $r = 0.10$, $p = 0.55$).

Granger-causality F-statistics were significantly higher in IwHS than in NT participants in both directions of prediction (Figure 2c). Specifically, F-statistics for predicting IR angular velocity from HA angular velocity were higher in IwHS than in NT participants (median [IQR]: 33.43 [19.03 - 64.49] vs. 12.15 [6.79 - 17.29], respectively; $p < 0.0001$). F-statistics for predicting HA angular velocity from IR angular velocity were also higher in IwHS than in NT participants (median [IQR]: 15.76 [8.15 - 23.89] vs. 7.01 [3.17 - 13.43], respectively; $p < 0.01$). Neither direction of Granger

prediction was associated with FMUE scores (HA→IR: $r = 0.08$, $p = 0.62$; IR→HA: $r = -0.02$, $p = 0.91$). Within both groups, F-statistics were higher for HA→IR than for IR→ HA prediction (NT: $p < 0.01$; IwHS: $p < 0.01$).

IwHS participants tended to have greater representation of IR angles above 90°. Figure 2d illustrates the differences in paired angular-position distributions between the IwHS and NT participants, where each pixel represents a specific combination of HA and IR angles, and therefore a distinct region of the joint-angle space. Nine joint-angle combinations were significantly overrepresented in IwHS relative to NT participants, forming a cluster characterized by $IR > 90°$. In contrast, the 12 underrepresented combinations were concentrated at $IR < 60°$. Within the overrepresented region, the distribution also appeared to extend along a shallow negative slope, suggesting that greater IR was associated with greater HA across this region of the joint-angle space.

We observed a similar pattern in the paired angular-velocity distributions (Figure 2e). Ten velocity combinations were significantly overrepresented in IwHS, forming a cluster that followed a negative diagonal, which would represent coordinated patterns of HA and IR velocities. There were conversely 32 velocity combinations that were underrepresented in IwHS and were distributed primarily across the remaining regions of the joint-velocity space. To further characterize how this movement pattern evolved through the HA-IR joint-angle space, we examined coupling fields or the distribution of angular velocity directions at each joint angle configuration (Figure 2f). NT participants revealed significant asymmetries in velocity direction aligned with the expected synergy at six joint angle configurations, although none occurred within

their highest-probability areas. IwHS data featured significant asymmetries aligned with the expected synergy at 17 configurations, with most occurring in regions that were frequently occupied.

3.2 Humeral Elevation Coupling with Elbow Flexion

Weighted correlations between HE and EF joint angles were significantly higher in IwHS than in NT participants (median [IQR]: 0.38 [0.22 - 0.55] vs. −0.01 [−0.12 - 0.09], respectively; $p < 0.0001$; Figure 3b). The strength of this relationship was associated with FMUE scores ($r = -0.34$, $p = 0.04$), with stronger correlations observed at lower FMUE scores. HE-EF angular velocity correlations were also higher in IwHS than in NT participants (median [IQR]: 0.25 [0.06 - 0.45 vs. 0.07 [−0.06 - 0.22], respectively; $p < 0.01$), although these correlations were not significantly associated with FMUE score ($r = -0.29$, $p = 0.09$).

Granger-causality F-statistics were significantly higher in IwHS than in NT participants when HE angular velocity was used to predict EF angular velocity (median [IQR]: 8.13 [5.02 - 16.09] vs. 4.61 [3.66 vs. 6.01], respectively; $p < 0.01$; Figure 3c). The IwHS group's F-statistics did not relate to FMUE ($r = -0.03$, $p = 0.88$). Conversely, F-statistics for predicting HE angular velocity from those of EF did not differ between IwHS and NT participants (median [IQR]: 6.42 [3.46 - 10.82] vs. 5.19 [3.58 - 7.56], respectively; $p = 0.38$). Here too, the F-statistics of the IwHS did not relate to FMUE ($r = -0.12$, $p = 0.49$).

Differences in the paired angular distributions reveal distinct regions of altered HE-EF joint configurations in IwHS participants (Figure 3d). Each pixel represents

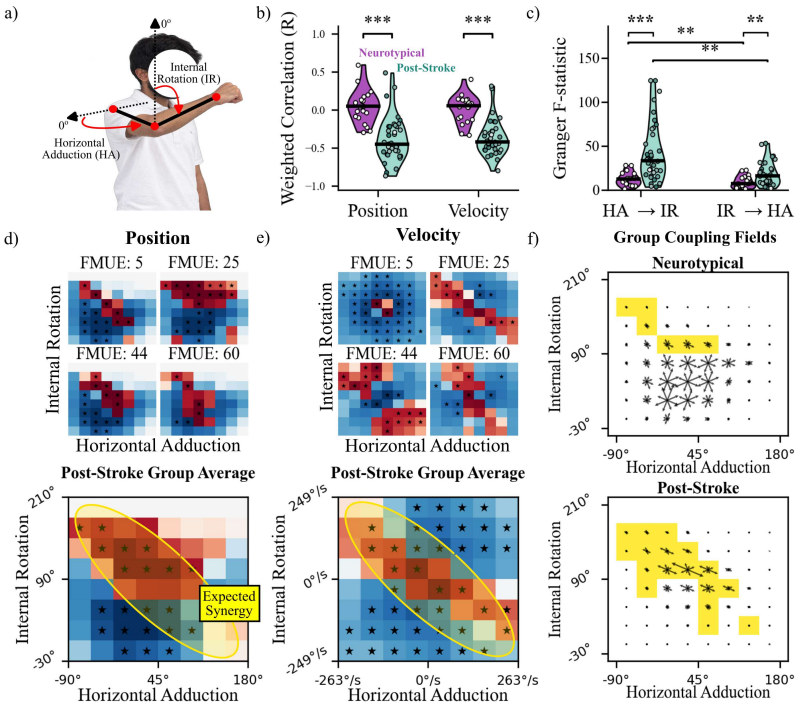


Fig. 2 a) **Horizontal adduction (HA) and internal rotation (IR) coupling.** b) Pearson weighted correlation between neurotypical (NT; magenta) and individuals with a history of stroke (IwHS) groups in joint angles and angular velocities distributions. Individual dots are shaded darker to correspond to FMUE score (0 = dark teal, 66 = white). c) Granger causality F-statistics between groups in both lead-lag combinations. d-e) Paired distribution differences between IwHS and NT participants for joint angles (d) and angular velocities (e), with red indicating overrepresentation and blue underrepresentation. Color scale and limits are consistent with Figure 1. Differences for four IwHS participants spanning FMUE scores 5-60 are shown first, with significant differences marked by stars, followed by the averaged post-stroke group differences. The hypothesized synergy is highlighted in yellow. f) Coupling field where the distribution of velocity direction vectors are shown in various regions of the joint angle space, where the arrow length indicates probability. Yellow highlighted pixels note significant asymmetry in the direction distribution along the hypothesized synergies.

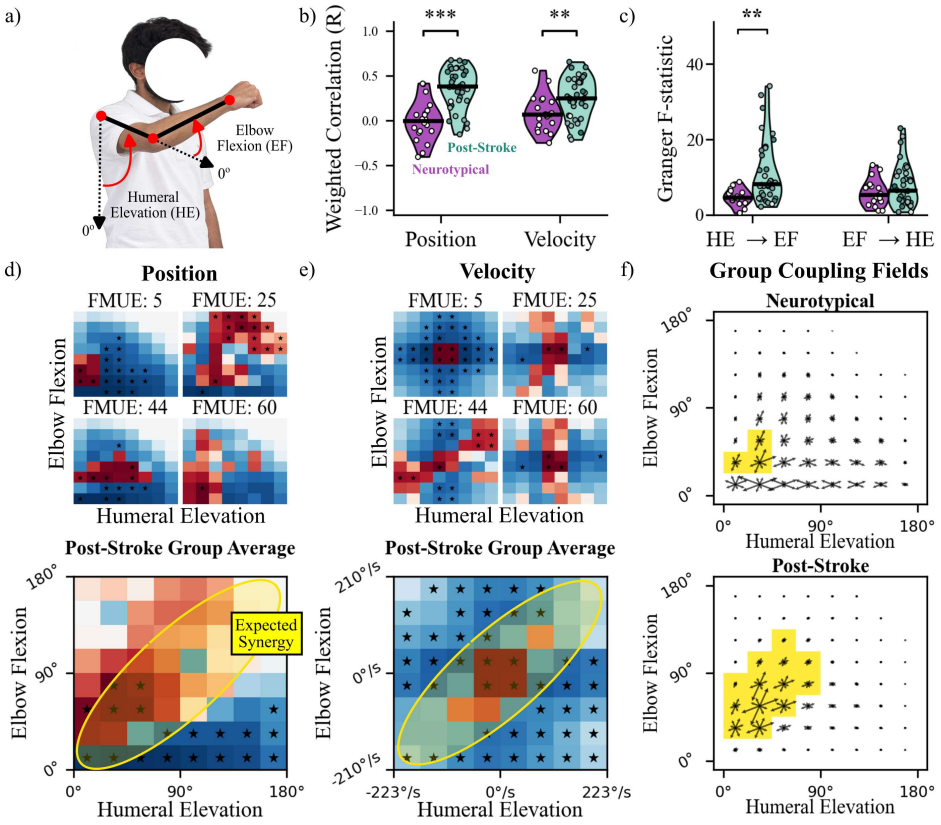


Fig. 3 a) **Humeral elevation (HE) and elbow flexion (EF) coupling.** b) Pearson weighted correlation coefficients in paired angular and angular velocity distributions of HE and EF of participants from the neurotypical (NT; magenta) and individuals with a history of stroke (IwHS; teal) groups. Dot darkness corresponds to impairment severity as measured by FMUE. c) Granger causality F-statistics between groups when testing both directions of predictive precedence. d-e) Differences in paired distributions between IwHS and NT participants for joint angles (d) and angular velocities (e). Red and blue indicate over- and underrepresented regions, respectively, with color scale and limits consistent with Figure 1. Four representative IwHS participants are shown relative to the NT reference, with significant differences marked by stars. Post-stroke group average differences presented, with the hypothesized synergy highlighted in yellow. f) Coupling field of velocity direction vectors in different regions of the joint angle space presented for both groups, where significant asymmetry following the hypothesized synergy pattern is shaded in yellow. The length of the arrows corresponds to likelihood of the velocity direction and joint configuration.

a specific combination of HE and EF angles. All eight configurations in the first row were underrepresented in IwHS, with six additional underrepresented configurations located in the bottom right region of the joint-angle space. Meanwhile, five configurations characterized by EF $> 45°$ and HE $< 90°$ were overrepresented in IwHS. Differences in the paired angular velocity distributions showed four overrepresented velocity combinations concentrated near the center of the distribution, while underrepresented combinations were primarily located in the bottom right and top left regions of the velocity space (Figure 3e). These underrepresented combinations correspond to movements of raising the humerus while extending the elbow or lowering the humerus while flexing the elbow.

Coupling fields further explore the directions of movement through the HE-EF joint-angle space (Figure 3f). In NT participants, three configurations in the lower left region noted significant directional asymmetries aligned with the positive diagonal, corresponding to movement around the resting arm with an extended elbow. In IwHS, 13 configurations revealed significant directional asymmetries, with the asymmetries generally following a positive diagonal through the most occupied configurations in the HE-EF joint-angle space.

3.3 Internal Rotation Coupling with Elbow Flexion

Internal rotation and EF angles showcased a significantly stronger negative correlation in the IwHS group than the NT group (median [IQR]: -0.24 [-0.33 - -0.07] vs. 0.01 [-0.18 - 0.13], respectively; $p < 0.01$; Figure 4b). The strength of this relationship was associated with FMUE score ($r = -0.57$, $p < 0.001$). Similarly, IR-EF angular

velocity correlations were lower in IwHS compared to the NT participants (median [IQR]: −0.09 [−0.26 - 0.03] vs. 0.08 [−0.08 - 0.13], respectively; $p < 0.01$), and were also associated with FMUE score ($r = -0.50$, $p < 0.01$).

Granger-causality F-statistics were higher in IwHS than in NT participants when IR angular velocities were used to predict those of EF (median [IQR]: 7.94 [3.00 - 13.80] vs. 3.08 [2.51 - 4.54], respectively; $p = 0.01$; Figure 4c). The F-statistics from the IwHS group did not relate with FMUE scores ($r = 0.05$, $p = 0.75$). In the opposite direction, F-statistics for predicting IR angular velocity from EF angular velocity did not differ significantly between IwHS and NT participants (median [IQR]: 8.19 [3.98 - 11.53] vs. 5.05 [2.73 - 6.08], respectively; $p = 0.08$). The IwHS groups' F-statistics were not associated with FMUE score ($r = -0.20$, $p = 0.24$).

Differences in the paired angular distributions revealed distinct regions of altered IR-EF joint configurations in IwHS participants (Figure 4d). Ten joint angle configurations were significantly overrepresented in IwHS and were clustered toward the higher IR region of the joint-angle space. There were also 14 configurations that were significantly underrepresented and clustered toward the lower IR regions of the joint-angle space. The paired angular velocity distributions revealed four significantly overrepresented velocity combinations near the center of the distribution and 41 combinations underrepresented in the upper right and lower left regions of the velocity space (Figure 4e). These underrepresented regions correspond to movements of IR with EF and external rotation with elbow extension. Coupling fields signified almost no directional asymmetries in the IR-EF joint-angle space (Figure 4f). No configurations in the NT group exhibited significant asymmetries aligned with the hypothesized IR-EF

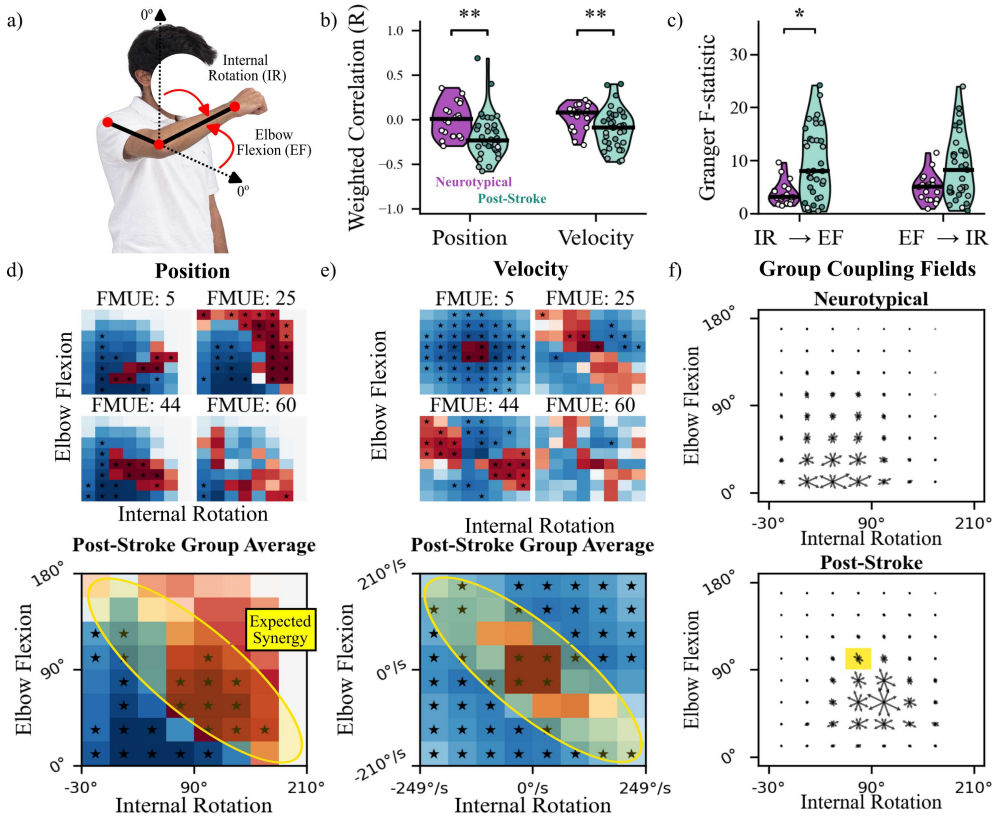


Fig. 4 a) **Internal rotation (IR) and elbow flexion (EF) coupling.** b) Pearson weighted correlations between paired angular and angular velocity distributions for participants in each of neurotypical (NT; magenta) and individuals with a history of stroke (IwHS; teal) and groups. Dot darkness denotes impairment severity based on FMUE. c) Granger causality F-statistics between groups when using one joint angle's velocity to predict the other and vice versa. d-e) Paired distribution differences between IwHS and NT participants for joint angles (d) and angular velocities (e), with red indicating overrepresented and blue indicating underrepresented regions. Color scale and limits are consistent with Figure 1. Four IwHS participants spanning the FMUE range are shown relative to the NT reference, with stars noting significant differences. Group-level differences are shown below, with the hypothesized synergy highlighted in yellow. f) Coupling field of the distribution of velocity direction vectors in pixels of the joint angle space for both NT and IwHS groups. The length of the arrows corresponds to likelihood of the velocity direction and joint configuration. A yellow shaded pixel indicates a significant asymmetry following the hypothesized pattern.

coupling direction. In the IwHS group, one configuration near the center of the joint-angle space had a significant directional asymmetry aligned with the hypothesized negative diagonal.

3.4 Humeral Elevation Coupling with Internal Rotation

Weighted correlations between HE and IR joint angles were similar in IwHS and NT participants during free exploration (median [IQR]: -0.25 [-0.35 - -0.14] vs. -0.29 [-0.34 - -0.19], respectively; $p = 0.35$; Figure 5b). The correlation was associated to FMUE scores ($r = -0.49$, $p < 0.01$). Similarly, HE-IR angular velocity correlations did not differ between IwHS and NT participants (median [IQR]: -0.15 [-0.26 - -0.04] vs. -0.15 [-0.23 - -0.12], respectively; $p = 0.88$) and were also not related to FMUE scores ($r = -0.36$, $p = 0.03$).

Granger-causality F-statistics did not differ between IwHS and NT participants in either direction of prediction (Figure 5c). F-statistics for predicting IR angular velocity from HE angular velocity were similar between IwHS and NT groups (median [IQR]: 10.26 [6.78 - 15.56] vs. 9.48 [5.88 - 12.53], respectively; $p = 0.36$). The F-statistics of IwHS did not relate with FMUE scores ($r = -0.07$, $p = 0.69$). The F-statistics also did not differ between IwHS and NT groups when using IR angular velocities to predict those of HE (median [IQR]: 11.26 [5.15 - 18.34] vs. 5.76 [3.87 - 9.76], respectively; $p = 0.10$) and the F-statistics from the IwHS group were not associated with FMUE scores ($r = 0.27$, $p = 0.11$).

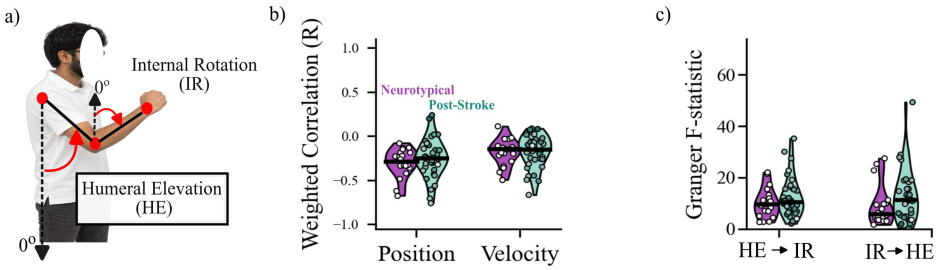


Fig. 5 a) **Humeral elevation (HE) and internal rotation (IR) coupling.** b) Weighted correlations between paired joint-angle and angular-velocity distributions for neurotypical (magenta) and individuals with a history of stroke (teal). Dot darkness indicates impairment severity based on FMUE scores. c) Granger F-statistics for predicting IR angular velocity from HE angular velocity and vice versa.

3.5 Horizontal Adduction Coupling with Elbow Flexion

Weighted correlations between HA and EF joint angles were significantly lower in IwHS than in NT participants (median [IQR]: −0.10 [−0.21 - 0.17] vs. 0.19 [0.07 - 0.32], respectively; $p < 0.001$; Figure 6b). Similarly, HA-EF angular velocity correlations were lower in IwHS than in NT participants (median [IQR]: −0.14 [−0.28 - 0.05] vs. 0.19 [0.08 - 0.31], respectively; $p < 0.0001$). Both angle and angular velocity correlations were associated with FMUE score ($r = 0.50$, $p < 0.01$ for angles; $r = 0.50$, $p < 0.01$ for angular velocities).

Granger-causality F-statistics did not differ significantly between IwHS and NT participants in either direction of prediction (Figure 6c). F-statistics for predicting EF angular velocity from HA angular velocity were similar between IwHS and NT groups (median [IQR]: 7.48 [3.48 - 11.75] vs. 4.31 [3.09 - 9.35], respectively; $p = 0.19$). The F-statistics of participants in the IwHS group were associated with FMUE scores

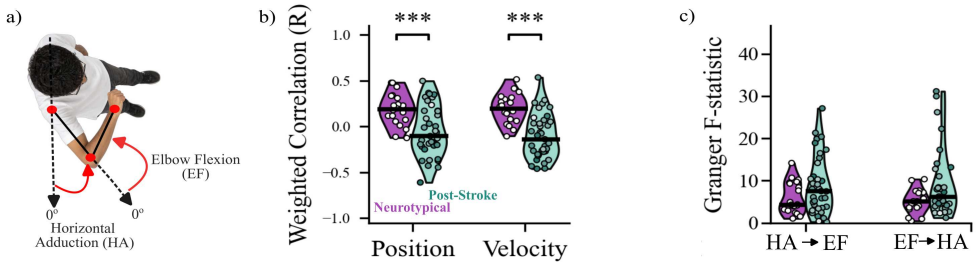


Fig. 6 a) **Horizontal adduction (HA) and elbow flexion (EF) coupling.** b) Weighted correlations between paired joint-angle and angular-velocity distributions for neurotypical (magenta) and individuals with a history of stroke (teal). Dot darkness indicates impairment severity based on FMUE scores. c) Granger F-statistics for predicting EF angular velocity from HA angular velocity and vice versa.

($r = -0.35$, $p = 0.03$). F-statistics for predicting HA angular velocity from EF angular velocity also did not differ between IwHS and NT participants (median [IQR]: 6.09 [4.08 - 11.44] vs. 5.04 [3.57 - 7.09], respectively; $p = 0.07$) and the IwHS's F-statistics were not associated with FMUE score ($r = -0.19$, $p = 0.27$).

3.6 Horizontal Adduction Coupling with Humeral Elevation

Weighted correlations between HA and HE joint angles did not differ between IwHS and NT participants (median [IQR]: 0.18 [0.05 - 0.29] vs. 0.14 [−0.01 - 0.22], respectively; $p = 0.09$; Figure 7b). The HA-HE angle correlation was related to FMUE scores in IwHS participants ($r = 0.36$, $p = 0.03$). HA-HE angular velocity correlations were significantly higher in IwHS than in NT participants (median [IQR]: 0.14 [0.06 - 0.26] vs. 0.06 [−0.04 - 0.13], respectively; $p = 0.03$), but were not associated with FMUE score ($r = 0.19$, $p = 0.25$).

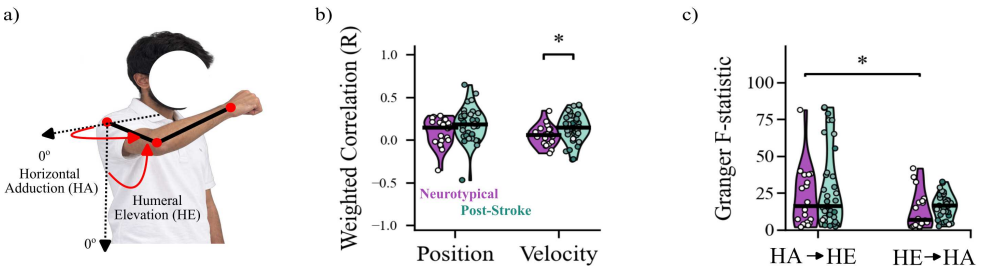


Fig. 7 a) **Horizontal adduction (HA) and humeral elevation (HE) coupling.** b) Weighted correlations between paired joint-angle and angular-velocity distributions for neurotypical (magenta) and individuals with a history of stroke (teal). Dot darkness indicates impairment severity based on FMUE scores. c) Granger F-statistics for predicting HE angular velocity from HA angular velocity and vice versa.

Granger-causality F-statistics did not differ between IwHS and NT participants in either direction of prediction (Figure 7c). When using angular velocities of HA to predict those of HE, the F-statistics were similar between IwHS and NT participants (median [IQR]: 15.94 [8.29 - 37.97] vs. 16.12 [5.48 - 35.97], respectively; $p = 0.56$) and were not associated with FMUE scores ($r = 0.11$, $p = 0.52$). Similarly, F-statistics for predicting HA angular velocity from HE angular velocity did not differ between IwHS and NT participants (median [IQR]: 16.29 [9.98 - 20.83] vs. 6.84 [3.48 - 19.23], respectively; $p = 0.17$) and were not associated with FMUE scores ($r = -0.00$, $p = 1.00$).

4 Discussion

In this work, we harnessed action likelihoods to characterize abnormal motor synergy patterns in kinematic distributions during unconstrained upper-extremity free

exploration following stroke. We first established a reference distribution from 20 NT participants, compared the distributions to 37 IwHS to identify correlations and pixel-level differences within paired kinematic distributions. This distribution-based approach provides a means of quantifying not only changes in the range of motion associated with stroke-related impairment, but also the altered coordination between joint degrees of freedom that may underlie AMS.

Comparison of the one-dimensional distributions revealed that IwHS exhibited similar HA distributions to NT participants, suggesting that overall range of HA was relatively preserved following stroke. This finding may be expected given that movement in this plane is less influenced by gravity and may therefore require less active torque to achieve. In contrast, IwHS presented with significantly lower HE, higher IR, and higher EF than NT participants. The reduction in HE was particularly evident at higher elevations, with the probability of occupying HE angles above $> 90°$ reduced in IwHS. This restricted elevation may reflect weakness, reduced motor control, or contracture at the shoulder, although the marginal distribution alone cannot distinguish between these mechanisms. The greater probability of flexed elbow positions may similarly reflect elbow contracture of AMS, but could also represent a compensatory strategy in which increased EF facilitates movement when shoulder elevation is limited. The increased IR is consistent with the flexed and internally rotated postures commonly observed following stroke and may reflect AMS, impaired activation of the external rotators, or soft-tissue restrictions. Importantly, these marginal distributions describe changes in joint-angle occupancy but cannot determine whether these

abnormalities arise independently or form altered coordination. We therefore examined paired distributions to characterize inter-joint coupling and identify distributional patterns consistent with AMS.

We first examined the relationship between HA and IR, which revealed significantly altered correlations in both angles and angular-velocity distributions in IwHS compared with NT participants ($p < 0.0001$). Granger causality analysis further uncovered significantly higher F-statistics in IwHS than in NT participants when predicting angular velocities in both directions, indicating an increased temporal predictive dependence between HA and IR. This bidirectional increase may reflect more biomechanical constraints, AMS, or a combination of both. For example, changes in the glenohumeral joint structurally and muscle imbalance following stroke could shift the relationship between the horizontal plane movements and humeral rotation. However, these biomechanical factors alone do not establish the source of the observed predictive dependence. Notably, F-statistics were higher when predicting IR angular velocity from HA angular velocity than when predicting HA angular velocity from IR angular velocity. This may indicate that changes in HA movement are more informative for predicting IR movement than vice versa. This asymmetry is consistent with the possibility of AMS. Together, these findings suggest that the relationship between HA and IR is altered following stroke, motivating our examination of their paired distribution structure.

Our pixel-level comparisons of HA and IR distributions uncovered an overrepresentation of more internally rotated positions in IwHS, with some participants also

exhibiting a downward-sloping pattern of significant differences. This pattern was particularly apparent in the example individuals with FMUE of 5 and 44. In contrast, the distribution of the individual with FMUE 25 appeared more consistent with a concurrent restriction toward internally rotated positions. These participant-specific findings raise the possibility that distinct combinations of deficits can contribute to the observed distributions. Moreover, the patterns we expect of AMS were more pronounced in paired angular velocity distributions, where overrepresented pixels followed a downward-sloping trajectory accompanied by underrepresented regions in opposing corners and curiously, in the middle two columns of the distribution. This structure may indicate that certain combinations of HA and IR velocities occur more frequently than expected from the NT reference group, while other combinations of movement are underrepresented. Specifically, central underrepresented regions in the middle columns might suggest a reduced ability to internally or externally rotate independently, let alone in movements opposite the synergy.

The coupling fields served to uncover movement asymmetries at each joint angle configuration. The NT participants' coupling fields of HA and IR contained traces of the expected AMS asymmetry. These were present at more internally rotated positions, potentially reflecting boundary effects. In IwHS, however, these asymmetries were more widespread across the range of motion, suggesting that altered coordination may extend throughout their movement. This spatially distributed pattern provides additional evidence that the relationship between HA and IR is altered following stroke. Although shoulder coordination is primarily discussed in relation to

shoulder abduction and external rotation, our findings highlight potentially important changes influencing external rotation from the horizontal-plane movements. One possible explanation is altered coordination among muscles contributing to these movements, including the pectoralis major and the rotator cuff. However, these observed kinematic patterns cannot establish specific muscle co-activation.

We found significantly higher correlations between HE and EF in IwHS than in NT participants in both angular-position and angular-velocity distributions. Within the IwHS group, these changes were also associated with FMUE scores, with more severely impaired participants exhibiting greater alterations in the relationship between these degrees of freedom. Several mechanisms may contribute to this finding. Biomechanically, elbow flexion shortens the effective lever arm of the upper limb and may reduce the shoulder torque required to elevate the arm, potentially allowing individuals with shoulder weakness to compensate through increased elbow flexion. Alternatively, the altered relationship may reflect abnormal muscle co-activation associated with post-stroke AMS, which the HE and EF are preferentially expressed together. We also observed significantly higher Granger causality F-statistics in IwHS when predicting EF angular velocity from HE angular velocity, whereas the reverse direction did not differ significantly between groups. This directional bias suggests that HE movement provides greater temporal information about subsequent EF movement post-stroke. However, this finding does not establish direct neural causation, and biomechanical or intent-related determinants may contribute. Nevertheless, the combination of altered correlations, associated with impairment severity, and direction-specific changes in

temporal predictability is consistent with altered coordination between HE and EF following stroke. This interpretation aligns with previous studies describing the coupling of shoulder abduction and elbow flexion in flexor synergies.

Pixel-level comparisons characterized the altered HE-EF relationship in IwHS. In the angular-position paired distributions, IwHS underrepresented the lowest EF angles, corresponding to greater elbow extension, potentially reflecting restricted extension associated with weakness, spasticity, or contracture. A slight positively sloped pattern was also apparent in the overrepresented and underrepresented regions, suggesting that differences in elbow-angle occupancy varied systematically with HE. We observed a similar pattern in the paired angular velocity distributions, where substantially large clusters of underrepresented pixels occurred in the upper-left and bottom-right regions, indicating that specific movements such as humeral elevation with elbow extension were less frequent in IwHS than in NT participants. Underrepresentation in portions of the central rows and columns ($0°/s$) may additionally point to reduced use of isolated HE and EF movements without the other. The coupling fields provided spatial information about where these altered relationships occurred across the workspace. Although some regions of directional asymmetry were also present in NT participants, substantially more pixels were significant in IwHS, predominantly in their most used areas of the workspace. This broader pattern suggests that the joint association was more prevalent across the workspace in IwHS. Taken together, the correlation, temporal-prediction, and pixel-level findings indicate that the relationship between HE and EF is altered following stroke and that these changes can be characterized during free exploration without prescribing specific reaching trajectories.

Paired distributions of IR and EF revealed significantly lower correlations in IwHS than in NT participants in both the angular-position and angular-velocity distributions. Notably, the relationship between individuals IR-EF correlations and FMUE scores was negative for both distributions ($p < 0.01$), indicating that correlations became more positive with increasing impairment severity. Although the IR-EF correlation was negative at the group-level, a couple participants with severe impairment exhibited positive correlations. These findings suggest that the relationship between IR and EF varies within IwHS with impairment severity, potentially reflecting interactions between abnormal coordination and an individual's biomechanical constraints. One possibility is that individuals with moderate impairment retain or rely on a consistent coordination pattern that may facilitate gross upper-extremity movements. Meanwhile in individuals with more severe impairments, weakness, restricted range of motion, contractures, or other motor deficits may impose or even reverse this relationship. Importantly, the Granger causality analysis revealed significantly higher F-statistics in IwHS when predicting EF angular velocity from IR angular velocity, with no significant group difference in the reverse direction. This finding raises the possibility that a directional component of inter-joint coordination persists following stroke, consistent with AMS. However, the lack of widespread directional asymmetries in the coupling fields suggests that this temporal relationship is not expressed as a consistent spatial pattern. Instead, individual limitations and compensatory strategies may substantially influence the observed distributions, particularly in participants with more severe impairments. Thus, the IR-EF relationship may reflect a combination of

directional coordination and impairment-specific constraints rather than a uniform post-stroke synergy.

Previous studies have demonstrated a relationship between shoulder abduction loading and external rotation in individuals post-stroke, typically by manipulating gravity support during planar reaching or isometric force matching and examining the resulting changes in kinematics and muscle activity [34, 35]. In contrast, our 3D free exploration task did not ascertain significant differences between IwHS and NT participants in HE-IR correlations for either joint angles or angular velocities. Notably, both groups had significant nonzero correlations, suggesting that the relationship between HE and IR is also present during typical movement and is not unique to post-stroke impairment. The absence of group differences further posits that this relationship is relatively preserved in our task, in contrast to the altered relationships observed for other joint pairs. The baseline correlations may reflect biomechanical constraints of the glenohumeral joint, typical neural coordination of shoulder movement, or a combination of these. Beyond this, differences in task demands may explain the contrast with previous findings. Unlike planar movements, our free exploration task did not limit shoulder elevation to any particular plane where the associated abduction load is dependent on the horizontal adduction and percent gravity support. It is also possible that, under the free-exploration conditions, the nonzero relationship observed in NT participants reflected a preferred movement strategy rather than underlying biomechanical or neurological constraint, whereas a similar relationship in IwHS may have been influenced by pathological restrictions toward the same pattern. Consistent with the correlation results, we found no group differences in Granger causality

F-statistics in either direction of angular-velocity prediction, providing no evidence of altered predictive dependence between HE and IR following stroke. Together, these findings may indicate that the relationship observed during 3D free exploration is not uniquely associated with post-stroke impairment, but may instead reflect coordination patterns common to both populations.

Compared with NT participants, IwHS exhibited lower correlations between HA and EF in both the angular-position and angular-velocity distributions suggesting an altered relationship between horizontal planar shoulder movement and elbow flexion. This may reflect differences in movement strategy, compensation from other deficits, etc. as correlations alone cannot establish a specific reason. Notably, within the IwHS group, both correlations were associated with FMUE scores such that low scoring participants had more negative correlations. This association suggests that the change in inter-joint relationship may be related to AMS, weakness, restricted joint mobility, and compensatory movement strategies. More severe impairment may include greater structural or functional limitations that constrain the combinations of shoulder and elbow movements, impacting the observed correlations. In contrast to these results, lead-lag analysis revealed no differences in F-statistics between the IwHS and NT participants in either predictive direction. Thus, we found no evidence of altered temporal predictive dependence between their angular velocities relative to the NT group. Because EF is a distal degree of freedom that may be influenced by multiple proximal joints and movement constraints, this discrepancy may reflect intermediate influences from other joints. Further investigation of multijoint relationships may

therefore be necessary to determine how HA interacts with EF to produce the observed distributional changes.

Correlations between HA and HE did not differ significantly between IwHS and NT participants. Although a statistically significant difference was observed in the angular-velocity distributions, the effect size was small ($|r| < 0.1$), suggesting that the magnitude of this difference was limited. Consistent with this finding, Granger causality analysis revealed no significant group differences in F-statistics in either direction of angular-velocity prediction, providing no evidence of altered temporal predictive dependence between these degrees of freedom following stroke. Together, these results suggest that the relationship between HA and HE remains relatively similar between IwHS and NT participants during free exploration, with little evidence of association. One possible explanation is that both movements can be performed with some degree of independence, allowing individuals to explore these dimensions without a strong constraint. These findings provide a useful reference for understanding which inter-joint relationships are preserved post-stroke.

Although our findings provide evidence of altered inter-joint relationships consistent with possible AMS, particularly between HA-IR and HE-EF, several limitations should be considered. First, the unstructured nature of the free-exploration task may introduce variability in the movements performed by individuals. Although all participants received the same instructions, they may have interpreted the task differently, exploring different regions of the workspace and employing distinct movement trajectories. This variability, combined with the heterogeneity in post-stroke impairments, may have influenced the observed distributional patterns and limited the identification

of consistent group-level signatures. We also had a sizeable age-difference between the groups, which may have impacted interpretation of the instructions and the strength of the participants at baseline. Furthermore, the sample of 57 participants with 20 NT and 37 IwHS limits the generalizability of our findings and the ability to quantify individual differences across the spectrum of impairment. Future work should expand these datasets to determine whether the observed distributional patterns are reproducible in large age-matched cohorts and across different levels and types of impairment.

To our knowledge, this study is among the first to characterize inter-joint relationships during 3D upper-extremity free exploration following stroke using action likelihood analysis. We therefore began with pairwise joint distributions to identify potentially meaningful relationships while maintaining interpretability. However, pairwise analyses cannot fully characterize the multijoint nature of upper extremity movements, as the observed relationship may be modulated or influenced by other joints. For example, the relationship between HE and IR could depend on the planar orientation in HA. Future work should extend this framework to higher-dimensional distributions or other multivariate approaches that capture interactions among multiple joints while addressing the increased data requirements of those representations.

Importantly, patterns in this study cannot isolate AMS from other impairments that frequently coexist following stroke, including weakness, spasticity, contracture, and restricted range of motion yet. So far, these patterns should be interpreted as kinematic signatures consistent with altered coordination. Nevertheless, identifying

reproducible distributional signatures is an important step toward developing objective movement-imaging approaches that complement clinical assessment. Future work should investigate how individual distributional features relate to specific impairments using complementary assessments. These data could help establish which features are associated with particular impairments, how multiple deficits interact and whether the resulting profiles provide information relevant to personalized treatment selection. Further, these features should be related to functional outcomes. Because upper-extremity function involves coordinated movement across multiple joints, this work may also benefit from incorporating additional degrees of freedom to better characterize relationships between movement impairment and gross and fine motor function.

Finally, measurement uncertainty associated with the Kinect v2 may have influenced the observed joint distributions and inter-joint relationships. Markerless joint estimation can be affected by occlusion, pose ambiguity and tracking errors, particularly during rapid movements such as free exploration. In our data, we observed intermittent discontinuities in joint position estimates when the wrist or elbow moved in front of the body, resulting in high-frequency artifacts that propagated into the calculated joint angles. This was particularly important for the study's analysis because such artifacts could introduce false correlations between joint angles and potentially be misinterpreted as AMS. We therefore conservatively limited the analysis to frequencies below 1.5 Hz, at which these discontinuities were substantially attenuated. While this approach reduced the influence of tracking artifacts, it also restricted our analysis to lower-frequency movement patterns and prevented examination of higher-frequency

components of movement, including fine-motor behaviors. The observed joint distributions and inter-joint relationships should be interpreted as reflecting lower frequency coordination patterns.

Modern monocular camera-based markerless tracking algorithms may help address these limitations by providing improved precision for upper-extremity joint estimation and enabling tracking of previously difficult-to-measure movements, such as finger flexion and wrist supination, expanding the capabilities of markerless motion capture [36]. Future studies could incorporate these approaches to extend the study's framework beyond the four joint angles here. Adding additional degrees of freedom could provide a more comprehensive understanding of how post-stroke movement patterns relate to both gross upper-extremity coordination and fine motor control.

5 Conclusion

In this study, we applied action likelihoods during three-dimensional free exploration to characterize upper-extremity movement patterns and altered inter-joint coordination in individuals with a history of stroke. By comparing marginal and paired distributions of horizontal adduction, humeral elevation, internal rotation, and elbow flexion between individuals post-stroke and neurotypical participants, we identified joint-specific changes in movement likelihood and converging evidence of altered coordination across correlation analyses, temporal-predictability, and regional differences in paired distributions. Our findings suggest altered relationships between horizontal adduction and external rotation, as well as between humeral elevation and elbow flexion, while the relationship between humeral elevation and internal rotation appeared

relatively preserved under the tested conditions. These results demonstrate the value of examining multidimensional distributions together with their temporal and spatial structure to characterize post-stroke movement abnormalities.

Broadly, action-likelihood analysis offers a potential framework for quantifying movement signatures associated with abnormal motor synergies and other post-stroke motor deficits during unconstrained movement. Such signatures could eventually support more objective movement assessment, help identify individual patterns of inter-joint coordination, and guide targeted rehabilitation strategies aimed at improving coordination. However, the observed patterns cannot be attributed to abnormal motor synergies alone as weakness, spasticity, and other impairments may contribute. Future work should independently characterize these deficits, investigate their contributions to individual movement signatures, and establish relationships with functional outcomes and rehabilitation response.

Supplementary information. Extended versions of Figures 5-7 including analyses on paired probability distribution differences and coupling fields can be found in the supplementary material available at: PattonRoboticsLab/Supplementary_Srivatsa_JNER2026

Acknowledgements. The authors thank Partha Ryali and all the members of the RoboticsLab for their support and ideas, the Shirley Ryan AbilityLab, and the Northwestern and UIC IRBs.

Declarations

- Funding This work was supported in part by NICHD under grant 1F30HD122382-01, in part by NIDILRR under Grant 90REGE0005-01 and in part by NIH under Grant R01NS053606.
- Conflict of interest/Competing interests The authors declare no conflicts of interest or competing interests.
- Ethics approval and consent to participate All 57 participants in the study provided informed consent to participate in their respective studies, which were approved by the Northwestern University Institutional Review Board (STU00216158, STU00216062, STU00215000, STU00220740, STU00218538).
- Consent for publication All authors consent to this manuscript's publication.
- Data availability The datasets used and/or analysed during the current study are available from the corresponding author on reasonable request.
- Materials availability Not applicable.
- Code availability The scripts used during the current study are available from the corresponding author on reasonable request.
- Author contribution AVS helped collect data, developed the action likelihood framework, analyzed the results, and drafted the manuscript. AR contributed to data collection and analysis and helped plan validation approaches. CC helped recruit participants and perform clinical assessments. VW, BB, AC, and MC contributed to kinematic analysis and figure generation. NRA helped recruit participants and provided guidance on distribution analysis methods. RJC provided expertise in contextualizing the results and processing markerless motion-tracking data. JLP

conceived the study, supervised the research, analysis, and interpretation of outcomes, and secured funding. All authors reviewed and edited the manuscript and approved the final version.

References

[1] Khan, F. *et al.* Prediction of Factors Affecting Mobility in Patients with Stroke and Finding the Mediation Effect of Balance on Mobility: A Cross-Sectional Study. *International Journal of Environmental Research and Public Health* **19**, 16612 (2022).

[2] McPherson, J. G. *et al.* Progressive recruitment of contralesional cortico-reticulospinal pathways drives motor impairment post stroke. *The Journal of Physiology* **596**, 1211–1225 (2018). URL https://onlinelibrary.wiley.com/doi/abs/10.1113/JP274968. _eprint: https://onlinelibrary.wiley.com/doi/pdf/10.1113/JP274968.

[3] Grefkes, C. & Fink, G. R. Recovery from stroke: current concepts and future perspectives. *Neurological Research and Practice* **2**, 17 (2020). URL https://www.ncbi.nlm.nih.gov/pmc/articles/PMC7650109/.

[4] Shah, S. K., Harasymiw, S. J. & Stahl, P. L. Stroke Rehabilitation: Outcome Based on Brunnstrom Recovery Stages. *The Occupational Therapy Journal of Research* **6**, 365–376 (1986). URL https://doi.org/10.1177/153944928600600604.

[5] Gladstone, D. J., Danells, C. J. & Black, S. E. The Fugl-Meyer Assessment of Motor Recovery after Stroke: A Critical Review of Its Measurement Properties. *Neurorehabilitation and Neural Repair* **16**, 232–240 (2002). URL https://doi.org/10.1177/154596802401105171.

[6] Karbasforoushan, H., Cohen-Adad, J. & Dewald, J. P. A. Brainstem and spinal cord MRI identifies altered sensorimotor pathways post-stroke. *Nature Communications* **10**, 3524 (2019). URL https://www.nature.com/articles/s41467-019-11244-3.

[7] Portilla-Jiménez, M., Yang, Y., Roh, J., Rymer, W. Z. & Li, S. Post-Stroke Abnormal Synergies Are a Resultant Behavior of the Interplay of Weakness, Spasticity, and Environmental Demands. *Neurorehabilitation and Neural Repair* (2026).

[8] McMorland, A. J. C., Runnalls, K. D. & Byblow, W. D. A Neuroanatomical Framework for Upper Limb Synergies after Stroke. *Frontiers in Human Neuroscience* **9**, 82 (2015). URL https://www.ncbi.nlm.nih.gov/pmc/articles/PMC4329797/.

[9] Twitchell, T. E. The Grasping Deficit in Infantile Spastic Hemiparesis. *Neurology* **8**, 13–13 (1958). URL https://www.neurology.org/doi/10.1212/wnl.8.1.13.

[10] McPherson, L. M. & Dewald, J. P. Differences between flexion and extension synergy-driven coupling at the elbow, wrist, and fingers of individuals with chronic hemiparetic stroke. *Clinical neurophysiology : official journal of the International Federation of Clinical Neurophysiology* **130**, 454–468 (2019). URL https://www.

ncbi.nlm.nih.gov/pmc/articles/PMC7856836/.

[11] FACCIORUSSO, S. *et al.* Muscle synergies in upper limb stroke rehabilitation: a scoping review. *European Journal of Physical and Rehabilitation Medicine* **60**, 767–792 (2024). URL https://www.ncbi.nlm.nih.gov/pmc/articles/PMC11558461/.

[12] Pandian, S., Arya, K. N., Kumar, V. & Joshi, A. K. Synergy-Based Motor Therapy Inducing Favorable Changes in Motor Function Components among Poststroke Subjects: A Single-Group Study. *Journal of Neurosciences in Rural Practice* **13**, 261–269 (2022). URL https://www.ncbi.nlm.nih.gov/pmc/articles/PMC9187400/.

[13] Khorasani, A. *et al.* Wearable Myoelectric Interface for Neurorehabilitation (MINT) to Recover Arm Function: a Randomized Controlled Trial (2025).

[14] Ellis, M. D., Carmona, C., Drogos, J. & Dewald, J. P. A. Progressive Abduction Loading Therapy with Horizontal-Plane Viscous Resistance Targeting Weakness and Flexion Synergy to Treat Upper Limb Function in Chronic Hemiparetic Stroke: A Randomized Clinical Trial. *Frontiers in Neurology* **9** (2018). URL https://www.frontiersin.org/journals/neurology/articles/10.3389/fneur.2018.00071/full.

[15] Lang, C. E., Bland, M. D., Bailey, R. R., Schaefer, S. Y. & Birkenmeier, R. L. Assessment of upper extremity impairment, function, and activity after stroke:

foundations for clinical decision making. *Journal of Hand Therapy* **26**, 104–115 (2013). URL https://www.jhandtherapy.org/article/S0894-1130(12)00074-9/abstract.

[16] Poole, J. L. & Whitney, S. L. Assessments of Motor Function Post Stroke: A Review. *Physical & Occupational Therapy In Geriatrics* **19**, 1–22 (2001). URL https://doi.org/10.1080/J148v19n02_01.

[17] Da Gama, A., Fallavollita, P., Teichrieb, V. & Navab, N. Motor Rehabilitation Using Kinect: A Systematic Review. *Games for Health Journal* **4**, 123–135 (2015). URL https://journals.sagepub.com/action/showAbstract.

[18] Unger, T. *et al.* Markerless Motion Capture in Routine Clinical Upper Limb Assessments: Validity and Insights Beyond Ordinal Scoring (2026). URL http://arxiv.org/abs/2607.23608. ArXiv:2607.23608 [cs.CV].

[19] Cornella-Barba, G., Okita, S., Li, Z. & Reinkensmeyer, D. J. Real-Time Sensing of Upper Extremity Movement Diversity Using Kurtosis Implemented on a Smartwatch. *Sensors* **24**, 5266 (2024). URL https://www.mdpi.com/1424-8220/24/16/5266. Number: 16.

[20] Lang, C. E. *et al.* Advancing Neurorehabilitation and Recovery Through Human Movement Quantification via Wearable Sensing. *Neurorehabilitation and Neural Repair* **40**, 746–759 (2026).

[21] Al-Ayyad, M., Owida, H. A., De Fazio, R., Al-Naami, B. & Visconti, P. Electromyography Monitoring Systems in Rehabilitation: A Review of Clinical Applications, Wearable Devices and Signal Acquisition Methodologies. *Electronics* **12**, 1520 (2023). URL https://www.mdpi.com/2079-9292/12/7/1520. Number: 7.

[22] Otte, K. *et al.* Accuracy and Reliability of the Kinect Version 2 for Clinical Measurement of Motor Function. *PLOS ONE* **11**, e0166532 (2016). URL https://journals.plos.org/plosone/article?id=10.1371/journal.pone.0166532.

[23] Scano, A., Molteni, F. & Molinari Tosatti, L. Low-Cost Tracking Systems Allow Fine Biomechanical Evaluation of Upper-Limb Daily-Life Gestures in Healthy People and Post-Stroke Patients. *Sensors* **19**, 1224 (2019). URL https://www.mdpi.com/1424-8220/19/5/1224.

[24] Srivatsa, A. V. *et al.* Distribution Analysis for Diagnostics and Therapeutics of Motor Actions. *IEEE Journal of Biomedical and Health Informatics* **30**, 5437–5452 (2026). URL https://ieeexplore.ieee.org/document/11266891.

[25] Scarpellini, A. *et al.* Tongue-Yoga: Precision Visual Feedback Rehabilitation Improves Tongue Agility. *IEEE Transactions on Neural Systems and Rehabilitation Engineering* **34**, 1352–1362 (2026). URL https://ieeexplore.ieee.org/document/11363165.

[26] Huang, F. C. & Patton, J. L. Individual patterns of motor deficits evident in movement distribution analysis. *IEEE ... International Conference on Rehabilitation Robotics : [proceedings]* **2013**, 6650430 (2013). URL https://www.ncbi.nlm.nih.gov/pmc/articles/PMC4453863/.

[27] Huang, F. C. & Patton, J. L. Movement distributions of stroke survivors exhibit distinct patterns that evolve with training. *Journal of NeuroEngineering and Rehabilitation* **13**, 23 (2016). URL https://doi.org/10.1186/s12984-016-0132-y.

[28] Wright, Z. A., Patton, J. L. & Huang, F. C. Energetics during robot-assisted training predicts recovery in stroke. *Annual International Conference of the IEEE Engineering in Medicine and Biology Society. IEEE Engineering in Medicine and Biology Society. Annual International Conference* **2018**, 2507–2510 (2018). URL https://www.ncbi.nlm.nih.gov/pmc/articles/PMC8767422/.

[29] Celian, C., Ryali, P., Wilson, V., Srivatsa, A. & Patton, J. L. A Wearable Anti-Gravity Supplement to Therapy Does Not Improve Arm Function in Chronic Stroke: A Randomized Pilot Trial. *Neurorehabilitation and Neural Repair* 15459683251338792 (2025). URL https://doi.org/10.1177/15459683251338792.

[30] Srivatsa, A. V. *et al. Abnormal Synergies and Muscle Weakness Identified in Stroke Survivors via Wrist Position Probability Distributions. 2025 International Conference On Rehabilitation Robotics (ICORR)*, 1147–1153 (2025). URL https://ieeexplore.ieee.org/document/11063041. ISSN: 1945-7901.

[31] Tomita, Y., Rodrigues, M. R. M. & Levin, M. F. Upper Limb Coordination in Individuals With Stroke: Poorly Defined and Poorly Quantified. *Neurorehabilitation and Neural Repair* **31**, 885–897 (2017).

[32] Levin, M. F., Liebermann, D. G., Parmet, Y. & Berman, S. Compensatory Versus Noncompensatory Shoulder Movements Used for Reaching in Stroke. *Neurorehabilitation and Neural Repair* **30**, 635–646 (2016).

[33] Çizmecioğulları, S., Mihçin, Ş. & Akan, A. On the Use of a Depth Camera for the Assessment of Upper Extremity Movements in Healthy Individuals. *Sensors* **26**, 1762 (2026). URL https://www.mdpi.com/1424-8220/26/6/1762.

[34] Roh, J., Rymer, W. Z., Perreault, E. J., Yoo, S. B. & Beer, R. F. Alterations in upper limb muscle synergy structure in chronic stroke survivors. *Journal of Neurophysiology* **109**, 768–781 (2013). URL https://doi.org/10.1152/jn.00670.2012.

[35] Ellis, M. D., Schut, I. & Dewald, J. P. A. Flexion synergy overshadows flexor spasticity during reaching in chronic moderate to severe hemiparetic stroke. *Clinical Neurophysiology* **128**, 1308–1314 (2017). URL https://www.sciencedirect.com/science/article/pii/S1388245717301840.

[36] Cotton, R. J., Firouzabadi, P. & Murray, W. Monocular Biomechanical Tracking of Fingers with Inverse Kinematics to Foundation Models (2026). URL http://arxiv.org/abs/2605.09258. ArXiv:2605.09258 [cs.CV].

Supplementary Files

This is a list of supplementary files associated with this preprint. Click to download.

- SupplementarySrivatsaJNER2026.pdf